Advanced Reduction in Power Redundant for High-Efficient Electrolytic-Capacitor-less Off-Line LED Driver

Guirguis Z. Abdelmessih
Electromechanical Eng. Dept.
University of Burgos
Burgos, Spain
gzakiguirguis@ubu.es

J. Marcos Alonso
Electrical Eng. Dept.
University of Oviedo
Gijon, Asturias, Spain
marcos@uniovi.es

Cesar Acero Marquina
Electromechanical Eng. Dept.
University of Burgos
Burgos, Spain
cacero@ubu.es

D. Camponogara
Federal University of Santa Maria
Santa Maria, RS, Brazil
douglas.camponogara@ufsm.br

Marco Antonio Dalla Costa
GEDRE – Intelligence in Lighting
Federal University of Santa Maria
Santa Maria, RS, Brazil
marcodc@gedre.ufsm.br

***Abstract*— This paper proposes a high-efficient electrolytic capacitor less off-line Light Emitting Diode (LED) driver that features a reduced power processing by the ripple reduction converter. The AC-DC driver is the Parallel Buck-Boost and Boost Converter (PB3C). The converter shows a high Power Factor (PF), low Total Harmonic Distortion (THD), and high efficiency. The two stages of the converter are not connected in cascade (series) mode, but they are connected in parallel mode, which produces a reduction in the circulating power in the converter. Furthermore, the IB3C is a two-stage driver that features two switches, one to control the LED current and the other to eliminate the ripple in the current. For further enhancement, the amount of circulating power is controlled in order to ensure a high efficiency. In this paper, the IB3C is analyzed, and a design methodology is proposed. A fully functioning simulation supplying an LED luminaire of 104.75 V/ 1.75 A is implemented. The simulation results of the IB3C shows a high PF equal to 0.99, a very small THD of 6 %, output current ripple reduction from of 100 % to 2 %, which represents a landmark in the ripple reduction methodologies.**

Keywords—parallel buck-boost and boost converter; ripple reduction; high efficiency LED driver; off-line LED drivers; power factor correction.

I. INTRODUCTION

Light-emitting-diodes (LEDs) are the leading technology in the lighting market, due to their powerful features, among others its longer lifetime, quoted to be between 25,000 to 50,000 hours with flux intensity over 70% of the initial flux (L70), their valid higher efficacy compared to other light sources by 250 lm/W or even 300 lm/W, in addition to a smaller size, fast response, robustness, reliability, high color rendering index, bendable feature if needed, etc. [1]-[12]. LEDs are DC devices which require a current-controlled power supply [13]-[15]. Besides the main duty of the LED driver to control the LED current, it has a secondary duty, which is to fulfil the standards, such as the IEC 61000-3-2 Class C standard [16] concerning the harmonic content of the input current, and the PF which must be higher than the level specified by the U.S. Energy Star program [17].

Several LED drivers topologies can be found in the literature, which can be classified as the following. Firstly, the single-stage converters providing a cheap and compact design that offers a trade-off operation between efficiency, ripple reduction, PF correction, and dimming. The commonly used single-stage converters are the buck and flyback converters. Secondly, the two-stage converters are the dominating drivers especially for medium to high power applications where the compliance with standards and regulations is a must. This is due to the fact that the two converters has different functionality, as one stage takes care of the PF and THD, and the second stage enhances the operation, by featuring a special ripple reduction technique, or providing an efficiency enhancement strategy by applying additional techniques as the Zero-Voltage-Switching (ZVS) or the Zero-Current-Switching (ZCS) [18]-[20]. Finally, the integrated converters show a hybrid solution between the small size and efficiency of the single-stage converters and the performance and features of the two-stage converters. Integrated converters are simply two-stage converters that share the controlled switch [21]-[27].

An innovative investigation line is the integrated parallel converters illustrated in [28]-[29], where the novel Integrated Parallel Buck-Boost and Boost converter (IPB3C) and the Magnetically Integrated Buck-Boost and Boost converter (MIPB3C) are presented. The converter shows great figures, namely, a high PF of 0.994, a very small THD of 10%, an output

This work is partially supported by the Spanish government under research projects PID2022-140750OA-I00 and TED2021-129372B-I00. Moreover, partially supported by the Brazilian government through EMBRAPII and CNPq funds.

This work is also supported in part by the Conselho Nacional de Desenvolvimento Científico e Tecnológico (CNPq) – Brasil, Coordenação de Aperfeiçoamento de Pessoal de Nível Superior – Brasil (CAPES/PROEX) – Finance Code 001, PRPGP/UFSM, INCT-GD, CAPES proc 23038.000776/2017-54, CNPQ proc 465640/2014-1, FAPERGS proc 17/2551-0000517-1, and CAPES PrInt. Finally, it is also partially supported by EMBRAPII.

current ripple of 6 %, and an efficiency of 92.62 % for the IPB3C. While the MIPB3C shows an even better efficiency of 93.65 % and a volume reduction of 14.65% in the magnetic components. Besides, the low capacitance needed allows for the elimination of the electrolytic capacitors and a longer driver lifetime. However, a room for improvement does exist. The integration of the switches decreases the number of components and provides less complication in control. However, the separation of those switches add more features, which are the complete ripple elimination and the decrease of the processed power amount.

In this paper, the PB3C is proposed to supply an LED luminary load of 183 W, providing high PF, low THD, almost negligible current ripple, high efficiency, and reduced power redundance. The operation of the converter is equivalent to two standalone converters working in parallel; at the input, a buck-boost converter operates as a Power Control (PC) stage and regulate the power factor, while the boost converter operates as a Ripple Reduction (RR) stage.

This paper is organized as follows. In Section II, the PB3C is presented. Section III shows the converter operational principles of the proposed PB3C. The mathematical and efficiency analysis are illustrated in section IV, while the simulation results are shown in section V. Finally, a brief conclusion of the contribution of this paper is presented in Section VI.

II. Derivation of the Proposed PB3C

The driver is operating as two converters (Buck-Boost and Boost) in parallel mode. Fig. 1 shows the electric diagram of the PB3C. The PC stage is the Buck-Boost converter that has its input connected to AC bridge while its output is the C_{BB}, this through a diode D_{BB} and an Inductor L_{BB} and a switch M_{BB}. In parallel to this converter there is the ripple reduction stage, a Boost converter, where the capacitor C_{Bo} is the input of this converter, while its output is the same output capacitor of the PC stage C_{BB}, also it has a diode D_{Bo} and an inductor L_{Bo} and a switch M_{BB}. The benefits gained from this structure are the following:

- No bulk capacitor needed; thus, it offers a longer lifetime, compact, and cheaper LED driver.
- The percentage of the processed power by the ripple reduction stage is now controlled and does not affect the ripple at the output, so it ensures a better efficiency compared to the conventional IPB3C [28].
- The ripple can be eliminated, nearly all, as the voltage of the Boost input capacitor can be controlled to exactly imitate the ripple in the output voltage capacitor.

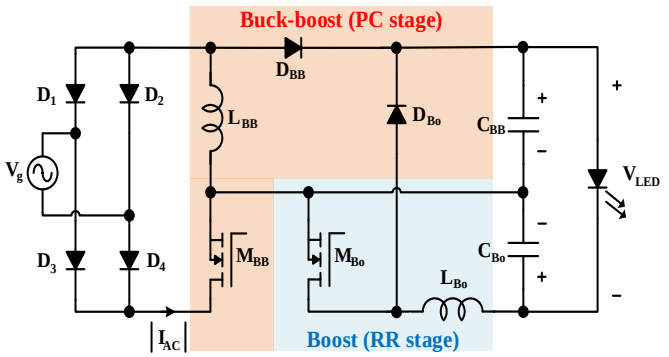

Fig. 1. Electric diagram of the PB3C.

III. Operational Principles of the Proposed PB3C

Since the proposed converter has two switches and because both have the same switching frequency, they can be analyzed together. Each switch has only two main states, on-state, and off-state. However, the DCM operation of both the buck-boost and boost converters splits the off-state into three intervals. Fig. 2, and Fig. 3 illustrate the main current waveforms within a high frequency switching period, and, the equivalent circuits respectively.

The following provides a concise explanation for each interval:

- Interval I

During this interval, the two main switches M_{BB} and M_{Bo} are turned on. While the switches are on, both inductors are charging. Thus, a current i_{BB} flows in the buck-boost input loop, coming from the AC grid to energize the buck-boost inductance. Meanwhile, a current i_{Bo} flows in the boost input loop, coming from the boost input capacitor, and energizing the boost inductor. The current is increasing linearly in both inductors.

- Interval II

This interval starts with the turn-off of the buck-boost switch. During this interval, the buck-boost inductor starts to de-energize, while the boost inductor is still energizing. The buck-boost inductor is de-energizing sending the power to the buck-boost capacitor through the buck-boost diode D_{BB}.

- Interval III

Interval III starts with the turn-off of the buck-boost switch. During this interval, the boost inductor starts to de-energize as well. The boost inductor is de-energizing delivering the power to the same buck-boost output capacitor through the boost diode D_{Bo}.

- Interval IV

This interval takes place when the inductor of the boost is completely discharged, while the inductor of the buck-boost is still de-energizing.

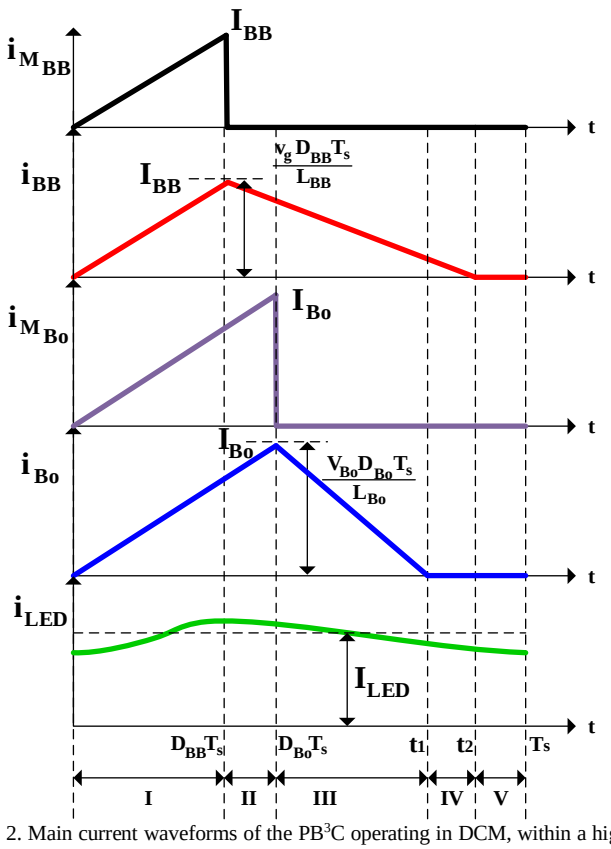

Fig. 2. Main current waveforms of the PB^{3}C operating in DCM, within a high-frequency switching period.

- Interval V

Finally, interval V represents the period when both inductors are fully discharged. However, the current going to the LED is continuous due to the output capacitor presence.

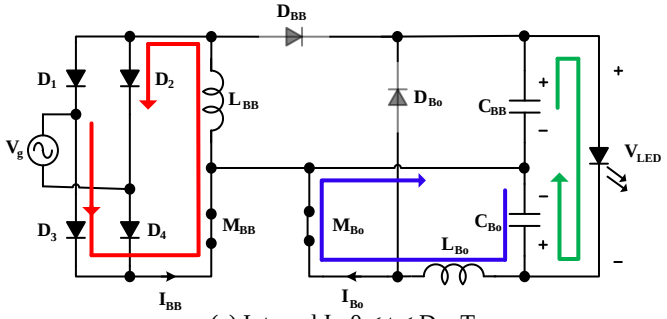

(a) Interval I : $0 < t < D_{BB} T_S$

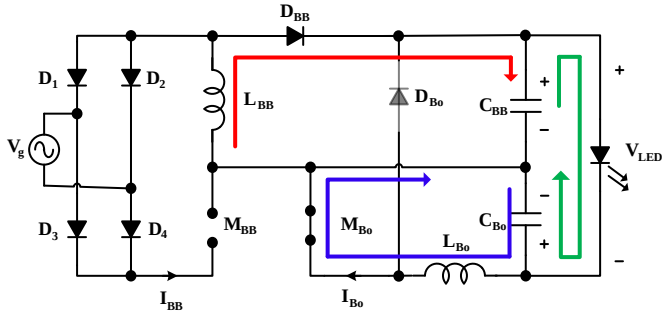

(b) Interval II : $D_{BB} T_S < t < D_{Bo} T_S$

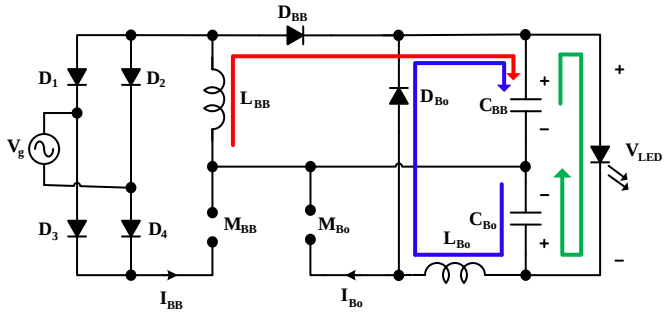

(c) Interval III : $D_{Bo} T_S < t < t_1$

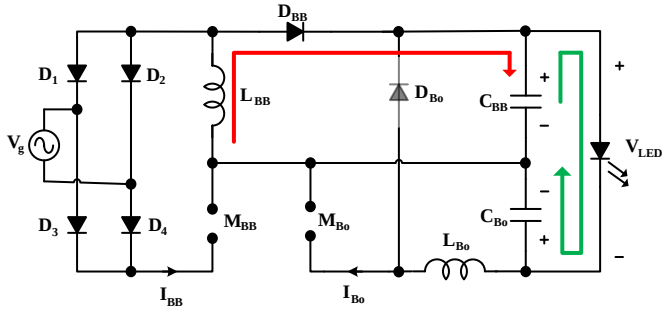

(d) Interval IV : $t_1 < t < t_2$

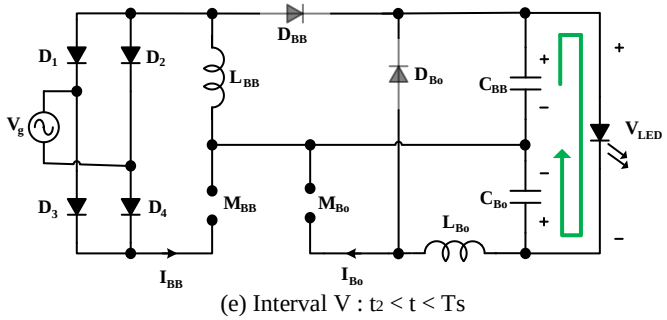

(e) Interval V : $t_2 < t < Ts$

Fig. 3. Equivalent circuits of the PB^{3}C operating in DCM.

IV. Mathematical Analysis and Efficiency Estimation of the PB3C

The operation equations presented for this converter are similar to the ones derived for the IPB3C in [28]. For the sake of simplicity, an ideal assumption is taken. The input voltage is considered to be an ideal sinusoidal line voltage waveform, expressed as $v_g(t) = V_g \sin(2\pi f_l t)$.

The converter contains three main power flows, that can be listed as the following:

- The input power (Grid power):

It is the power coming from the grid, which is expressed by the following equation:

$$P_{PC} = P_g = \frac{V_g^2 {D_{BB}}^2}{4 L_{BB} f_s} \tag{1}$$

Where P_g is the power of AC main, V_g is the grid peak voltage, D_{BB} is the buck-boost switch duty cycle, L_{BB} is the buck-boost inductance, and f_s is the switching frequency.

- RR stage power (Redundant Power):

It is the power handled by the RR stage and the power circulating in the converter, it is expressed by the following:

$$P_{RR} = \frac{V_{Bo}^2 {D_{Bo}}^2}{2 L_{Bo} f_s} \left(\frac{V_{BB}}{V_{BB} - V_{Bo}} \right) \tag{2}$$

Where V_{Bo} is the boost input voltage, L_{Bo} is the boost inductance, D_{Bo} is the boost switch duty cycle, and V_{BB} is the buck-boost output voltage.

- Output loop power:

It represents the power going out from the buck-boost capacitor to the LED added to the power going into the boost converter. Considering the converter in ideal conditions, the following relations of the output loop are found:

$$\begin{aligned} P_{BB} &= I_{LED} * V_{BB} = I_{LED} * V_{Bo} + I_{LED} * V_{LED} \\ &= P_{RR} + P_{LED} \end{aligned} \tag{3}$$

$$P_{LED} = P_{BB} - P_{RR} = P_{PC} \tag{4}$$

Thus, the input power and RR stage power can be expressed as the following:

$$\begin{aligned} P_{RR} &= I_{LED} * V_{Bo} \\ P_{PC} &= I_{LED} * V_{LED} \end{aligned} \tag{5}$$

Using (1), (2), and (5) a relationship between the buck-boost output voltage, and boost input voltage is found as the following:

$$V_{BB} V_{Bo} = \frac{V_g^2 L_{Bo} {D_{BB}}^2}{2 L_{BB} {D_{Bo}}^2} \tag{6}$$

An additional relationship between the buck-boost output voltage and the boost input voltage is found from the output loop, as follows:

$$V_{BB} = V_{Bo} + V_{LED} \tag{7}$$

Concerning the efficiency estimation, it will be calculated as a factor of the efficiency of each converter. In the proposed topology the percentage of the circulating power, the power handled by the boost converter, is defined by the DC value of the boost capacitor.

$$V_{Bo} = K * V_{LED} \tag{8}$$

$$P_{RR} = K * P_{LED} \tag{9}$$

Where K is the RR stage power sharing factor.

The total efficiency of the parallel integrated converter is found:

$$\eta_{total} = \frac{P_{LED}}{P_g} = \frac{\eta_{PC}}{1 + K * (1 - \eta_{RR})} \quad (10)$$

Where η_{total} is the total efficiency of the converter, η_{RR} is the efficiency of the RR stage (the boost converter), and η_{Pc} is the efficiency of the PC stage (the buck-boost converter).

In order to illustrate better the idea of parallel integration and its effect on the efficiency an example is studied. For this application a boost average voltage will be design equal to 30% of the LED voltage (32 Volts), which means that the k factor is equal to 0.3. It will be estimated that the efficiency of the buck-boost is equal to 90 %, and the efficiency of the boost is equal to 90 %. In this case the efficiency of the conventional cascaded two stages converter is equal to the product of both efficiencies, which is, 81 %. However, in the proposed converter the estimated efficiency can be found by applying those values in (10), and the efficiency is estimated to be equal to 87 %.

Creo que faltaría añadir aquí una sección explicando un poco cómo se hace el control de los interruptores y del circuito completo.

V. Simulation Results

A simulation for the proposed converter is made using PowerSim (PSIM) software. Fig. 4 shows the schematic of the PB3C of the PSIM simulation. The linear model to represent the LED is made using the following values for the threshold voltage and the dynamic resistance: $V_{th} = 82\,V$ and $R_d = 13\,\Omega$. The RMS value of the input voltage is equal to 110 V. Table I illustrates the parameters and limitations of the components of the converter.

TABLE I
Components of Proposed Prototype

Component	Value
EMI Filter Inductor	*2.58 mH*
EMI Filter Capacitor	*100 nF*
Buck-boost Inductance	$L_{BB} = 50\,\mu H$
Boost Inductance	$L_{Bo} = 10\,\mu H$
Buck-boost diode D_{BB}	$V_{rev} = 400\,V, I_{peak} = 12\,A$
Boost diode D_{Bo}	$V_{rev} = 160\,V, I_{peak} = 6\,A$
Buck-boost switch M_{BB}	$V_{blo} = 400\,V, I_{peak} = 12\,A$
Boost switch M_{Bo}	$V_{blo} = 200\,V, I_{peak} = 5\,A$
Output Buck-boost Capacitor C_{BB}	68 µF, 160 V
Intput boost Capacitor C_{Bo}	20 µF, 50 V

Fig. 5 shows the input voltage and current. The proposed topology ensures that the PF and THD are far below limitations, as can be seen from the pure sinusoidal input current waveform. The ideal conditions guaranteed by the simulation platform helped the proposed topology to reach almost zero THD and nearly unity PF, however, in the real application it is expected to have a small difference.

The LED voltage is the difference between buck-boost output voltage and the boost input voltage. Therefore, the ripples are also subtracted. The idea of this topology is to reduce the DC level of the boost converter as much as possible and to make its ripple equal to the ripple in the buck-boost voltage.

Fig. 6 shows the three main voltages, the output buck-boost voltage, the input boost voltage, and the LED voltage. Fig 6a shows the case where the ripple reduction technique is not active, this is, the case of the integrated converter where both switches are working with the same duty cycle. Fig. 6b shows the case for the same three voltages but when the ripple elimination technique is operating. As can be seen in Fig. 5a the ripple at the input of the boost converter is subtracted from the output buck-boost voltage ripple , but it is not enough to remove the ripple completely. When the ripple reduction is activated the ripple at the input boost capacitor is increased to eliminate the LED voltage ripple completely, as can be seen in Fig. 6b.

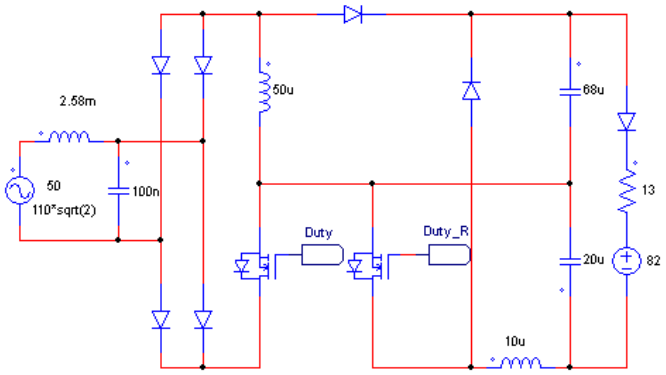

Fig. 4. PSIM circuit of the parallel buck-boost and boost LED driver.

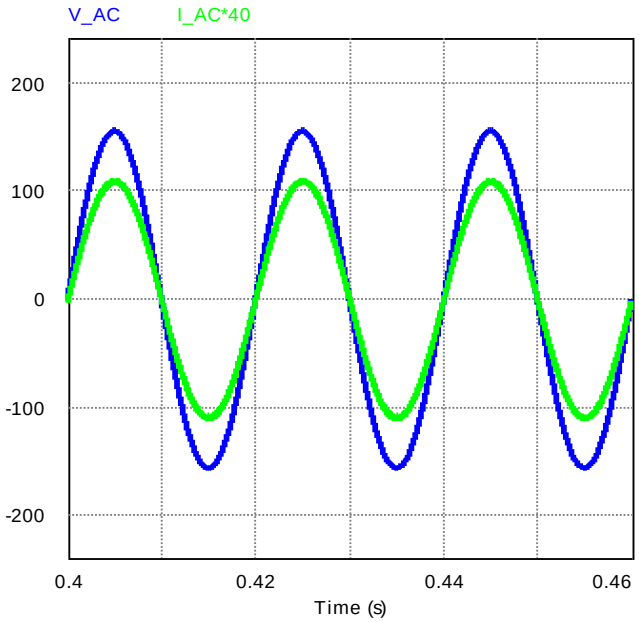

Fig. 5. AC main voltage (blue), AC main current (green).

Fig. 7 shows the LED current in the two cases with and without the ripple reduction technique. As can be seen, the low-frequency ripple in the case without the ripple reduction is equal to 100 %. However, when the ripple reduction technique is activated at instant 0.15 s, the ripple decreases as low as 2 %. Thus, it is far below the flicker recommended by IEEE1789-2015.

VI. Conclusions

This paper presents a novel efficient LED driver, which ensures high PF and low THD to be far below the limitation specified by IEC 61000-3-2 recommendation. Moreover, the converter ensures neglected LED current ripple using two low voltage capacitors with small capacitance, which lead to an electrolytic-capacitor-less driver. This is done by a two stage parallel converter, which is composed of a buck-boost converter operating as a PC stage and PFC stage, and a boost converter operating as RR stage. Furthermore, the proposed topology does not require any coupled inductors nor transformers, which means that a spike-less operation is ensured, and winding losses can be minimized. Regarding the power component, the proposed topology offers all these features by using two power

switches. Furthermore, the parallel features to control the percentage of the circulating power in the RR stage, allowing for an improved efficiency compared with the conventional cascade structure. Lastly, the converter shows a better control for the ripple of the LED current with even less power redundant in the converter.

Finally, a simulation for a 110 V, 50 Hz line input, and 104.75 V output, driving an LED luminaire of 182 W, has been designed to illustrate the application of the derived characteristics. Simulation results have proven that the harmonic content of the input current equals nearly zero, with nearly unity PF, so that the converter meets the IEC-61000-3-2 standard and U.S. Energy Star program requirements. Concerning the efficiency of the proposed driver, it is higher than the conventional cascaded converters and the IPB3C. If the conventional cascaded converter shows an efficiency of 81 %. The proposed topology shows a better efficiency as the boost converter handles only 30 % of the LED power, while the integrated version to eliminate a significant percentage from the ripple needs to circulate 70 % at least. Thus, using the previously estimated efficiencies of the buck-boost and boost converters, the PB^{3}C shows an efficiency of 87 %, which is 6 % higher than the conventional cascaded configuration.

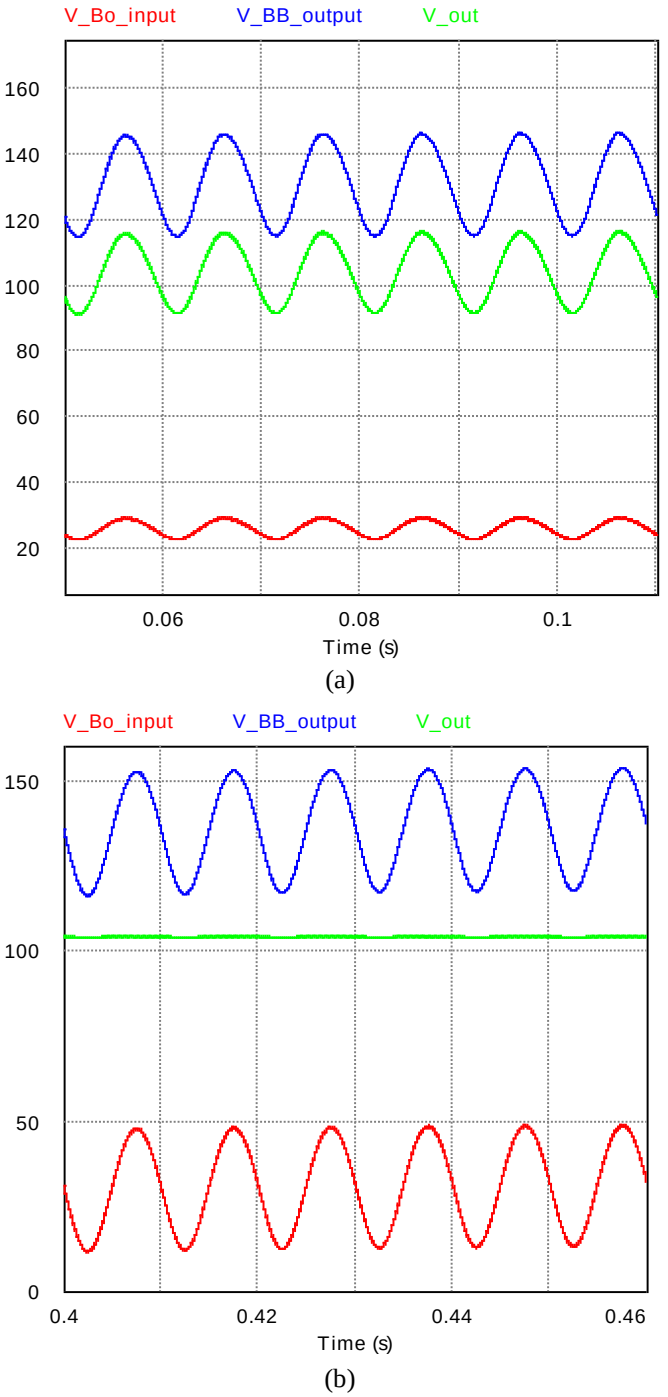

Fig. 6. Buck-boost output voltage (blue), boost input voltage (red), and LED voltage (green).

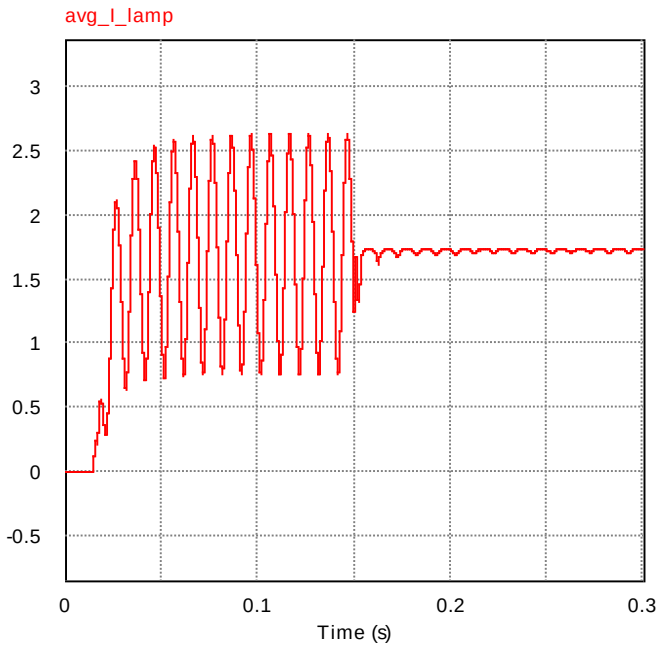

Fig. 7. LED current filtered from high-frequency ripple.

REFERENCES

[1] H. -J. Chiu, Y. -K. Lo, J. -T. Chen, S. -J. Cheng, C. -Y. Lin and S. -C. Mou, "A High-Efficiency Dimmable LED Driver for Low-Power Lighting Applications," in IEEE Transactions on Industrial Electronics, vol. 57, no. 2, pp. 735-743, Feb. 2010.

[2] Y. Wang, J. M. Alonso and X. Ruan, "A Review of LED Drivers and Related Technologies," in IEEE Transactions on Industrial Electronics, vol. 64, no. 7, pp. 5754-5765, July 2017.

[3] M. Arias, D. G. Lamar, J. Sebastian, D. Balocco and A. A. Diallo, "High-Efficiency LED Driver Without Electrolytic Capacitor for Street Lighting," in IEEE Transactions on Industry Applications, vol. 49, no. 1, pp. 127-137, Jan.-Feb. 2013.

[4] J. M. Alonso; "LED Lighting and Drivers," Amazon KDP, 2019.

[5] P. S. Almeida, D. Camponogara, M. Dalla Costa, H. Braga and J. M. Alonso, "Matching LED and Driver Life Spans: A Review of Different Techniques," in IEEE Industrial Electronics Magazine, vol. 9, no. 2, pp. 36-47, June 2015.

[6] D. G. Lamar, M. Fernandez, M. Arias, M. M. Hernando and J. Sebastian, "Tapped-Inductor Buck HB-LED AC–DC Driver Operating in Boundary Conduction Mode for Replacing Incandescent Bulb Lamps," in IEEE Transactions on Power Electronics, vol. 27, no. 10, pp. 4329-4337, Oct. 2012.

[7] Y. Wang, Y. Guan, K. Ren, W. Wang and D. Xu, "A Single-Stage LED Driver Based on BCM Boost Circuit and LLC Converter for Street Lighting System," in IEEE Transactions on Industrial Electronics, vol. 62, no. 9, pp. 5446-5457, Sept. 2015.

[8] A. Barroso, P. Dupuis, C. Alonso, B. Jammes, L. Seguier and G. Zissis, "A characterization framework to optimize LED luminaire's luminous efficacy," 2015 IEEE Industry Applications Society Annual Meeting, Addison, TX, 2015, pp. 1-8.

[9] R. Jaschke and K. F. Hoffmann, "Higher Light Efficacy in LED-Lamps by lower LED-Current," PCIM Europe 2016; International Exhibition and Conference for Power Electronics, Intelligent Motion, Renewable Energy and Energy Management, Nuremberg, Germany, 2016, pp. 1-5.

[10] R. L. Lin, Y. C. Chang and C. C. Lee, "Optimal Design of LED Array for Single-Loop CCM Buck–Boost LED Driver," in IEEE Transactions on Industry Applications, vol. 49, no. 2, pp. 761-768, March-April 2013.

[11] G. Z. Abdelmessih, J. M. Alonso and M. A. Dalla Costa, "Analysis, design, and experimentation of the active hybrid-series-parallel PWM dimming scheme for high-efficient off-line LED drivers," in IET Power Electronics, vol. 12, no. 7, pp. 1697-1705, 19 6 2019.

[12] R. L. Lin, J. Y. Tsai, S. Y. Liu and H. W. Chiang, "Optimal Design of LED Array Combinations for CCM Single-Loop Control LED Drivers," in IEEE Journal of Emerging and Selected Topics in Power Electronics, vol. 3, no. 3, pp. 609-616, Sept. 2015.

[13] R. A. Pinto, J. M. Alonso, M. S. Perdigão, M. F. da Silva and R. N. do Prado, "A New Technique to Equalize Branch Currents in Multiarray LED Lamps Based on Variable Inductors," in IEEE Transactions on Industry Applications, vol. 52, no. 1, pp. 521-530, Jan.-Feb. 2016.

[14] H. van der Broeck, G. Sauerlander and M. Wendt, "Power driver topologies and control schemes for LEDs," APEC 07 - Twenty-Second Annual IEEE Applied Power Electronics Conference and Exposition, Anaheim, CA, USA, 2007, pp. 1319-1325.

[15] G. Z. Abdelmessih, J. M. Alonso and W. Tsai, "Analysis and Experimentation on a New High Power Factor Off-Line LED Driver Based on Interleaved Integrated Buck Flyback Converter," in IEEE Transactions on Industry Applications, vol. 55, no. 4, pp. 4359-4369, July-Aug. 2019

[16] Electromagnetic Compatibility (EMC) - Part 3-2: Limits for Harmonic Current Emissions, IEC 61000-3-2: 2005, Nov. 2005.

[17] "ENERGY star program requirements for solid state lighting luminaries, version 1.3," U.S. Environ. Protection Agency, U.S. Dept. Energy, Washington, DC, USA, 2010.

[18] F. Zhang, J. Ni, and Y. Yu, "High power factor AC–DC LED driver with film capacitors," IEEE Trans. Power Electron., vol. 28, no. 10, pp. 4831–4840, Oct. 2013.

[19] Y. Wang, Y. Guan, D. Xu, and W. Wang, "A CLCL resonant DC/DC converter for two-stage LED driver system," IEEE Trans. Ind. Electron., vol. 63, no. 5, pp. 2883–2886, May 2014.

[20] J. -W. Yang and H. -L. Do, "High-Efficiency ZVS AC-DC LED Driver Using a Self-Driven Synchronous Rectifier," in IEEE Transactions on Circuits and Systems I: Regular Papers, vol. 61, no. 8, pp. 2505-2512, Aug. 2014.

[21] Gacio, D.; Alonso, J.M.; Calleja, A.J.; Garcia, J.; Rico-Secades, M., "A Universal-Input Single-Stage High-Power-Factor Power Supply for HBLEDs Based on Integrated Buck-Flyback Converter, " in Applied Power Electronics Conference and Exposition, 2009. APEC 2009. TwentyFourth Annual IEEE , vol., no., pp.570-576, 15-19 Feb. 2009.

[22] G. Z. Abdelmessih, J. M. Alonso and M. A. Dalla Costa, "Loss Analysis for Efficiency Improvement of the Integrated Buck–Flyback LED Driver," in IEEE Transactions on Industry Applications, vol. 54, no. 6, pp. 6543-6553, Nov.-Dec. 2018.

[23] Alonso, J.M.; Dalla Costa, M.A.; Ordiz, C., "Integrated Buck-Flyback Converter as a High-Power-Factor Off-Line Power Supply, " in Industrial Electronics, IEEE Transactions on , vo1.55, no.3, pp.1090-I 100, March 2008

[24] Y. Wang, J. Huang, W. Wang and D. Xu, "A single-stage single-switch LED driver based on integrated buck-boost circuit and Class E converter," 2015 IEEE Industry Applications Society Annual Meeting, Addison, TX, 2015, pp. 1-5.

[25] M. Wu, S. Li, S. Tan and S. Y. M. Wu, S. Li, S. Tan and S. Y. Hui, "Optimal Design of Integrated Magnetics for Differential Rectifiers and Inverters," in IEEE Transactions on Power Electronics, vol. 33, no. 6, pp. 4616-4626, June 2018.

[26] G. Z. Abdelmessih, J. M. Alonso, W. Tsai and M. A. Dalla Costa, "High-Efficient High-Power-Factor Off-Line LED Driver based on Integrated Buck and Boost Converter," 2019 IEEE Industry Applications Society Annual Meeting, Baltimore, MD, USA, 2019, pp. 1-6.

[27] K. Luewisuthichat, P. Boonprasert, C. Ekkaravarodome and A. Bilsalam, "Analysis and Implement DC-DC Integrated Boost-Flyback Converter with LED Street Light Stand-by Application," 2020 International Conference on Power, Energy and Innovations (ICPEI), Chiangmai, Thailand, 2020, pp. 197-200.

[28] G. Z. Abdelmessih, J. M. Alonso, N. d. S. Spode and M. A. D. Costa, "High-Efficient Electrolytic-Capacitor-Less Offline LED Driver With Reduced Power Processing," in IEEE Transactions on Power Electronics, vol. 37, no. 2, pp. 1804-1815, Feb. 2022

[29] G. Z. Abdelmessih, J. M. Alonso, I. B. Barboza and M. A. Dalla Costa, "Magnetically-Integrated Parallel Buck-Boost and Boost Converter as a High-Efficient High-Power-Density Off-Line LED Driver," 2023 IEEE Industry Applications Society Annual Meeting (IAS), Nashville, TN, USA, 2023, pp. 1-8